The Journal of Immunology

Foxp3$^+$ CD4 Regulatory T Cells Limit Pulmonary Immunopathology by Modulating the CD8 T Cell Response during Respiratory Syncytial Virus Infection

Ross B. Fulton, David K. Meyerholz and Steven M. Varga

J Immunol 2010; 185:2382-2392; Prepublished online 16 July 2010;
doi: 10.4049/jimmunol.1000423
http://www.jimmunol.org/content/185/4/2382

The Journal of Immunology is published twice each month by
The American Association of Immunologists, Inc.,
1451 Rockville Pike, Suite 650, Rockville, MD 20852

Print ISSN: 0022-1767 Online ISSN: 1550-6606.

Foxp3$^+$ CD4 Regulatory T Cells Limit Pulmonary Immunopathology by Modulating the CD8 T Cell Response during Respiratory Syncytial Virus Infection

Ross B. Fulton,* David K. Meyerholz,† and Steven M. Varga*,†,‡

Regulatory Foxp3$^+$ CD4 T cells (Tregs) prevent spontaneous inflammation in the lungs, inhibit allergic and asthmatic responses, and contribute to tolerance to inhaled allergens. Additionally, Tregs have previously been shown to suppress the CD8 T cell response during persistent virus infections. However, little is known concerning the role that Tregs play in modulating the adaptive immune response during acute respiratory virus infections. We show following acute respiratory syncytial virus (RSV) infection that Foxp3$^+$ CD4 Tregs rapidly accumulate in the lung-draining mediastinal lymph nodes and lungs. BrdU incorporation studies indicate that Tregs undergo proliferation that contributes to their accumulation in the lymph nodes and lungs. Following an acute RSV infection, pulmonary Tregs modulate CD25 expression and acquire an activated phenotype characterized as CD11a^{high}, CD44^{high}, CD43^{glyco+}, ICOS$^+$, and CTLA-4$^+$. Surprisingly, in vivo depletion of Tregs prior to RSV infection results in delayed virus clearance concomitant with an early lag in the recruitment of RSV-specific CD8 T cells into the lungs. Additionally, Treg depletion results in exacerbated disease severity, including increased weight loss, morbidity, and enhanced airway restriction. In Treg-depleted mice there is an increase in the frequency of RSV-specific CD8 T cells that coproduce IFN-γ and TNF-α, which may contribute to enhanced disease severity. These results indicate that pulmonary Tregs play a critical role in limiting immunopathology during an acute pulmonary virus infection by influencing the trafficking and effector function of virus-specific CD8 T cells in the lungs and draining lymph nodes. ***The Journal of Immunology*****, 2010, 185: 2382–2392.**

The respiratory tract forms a major mucosal interface with the external environment and is constantly exposed to inert foreign Ags and pathogens. Thus, the lungs must discriminate between innocuous and pathogen-derived Ags to limit chronic inflammation and maintain proper lung function. To do so, the respiratory system establishes a default anti-inflammatory state that requires a higher activation threshold for pathogen-associated danger signals than for nonmucosal surfaces (1). Once the threshold for innate immune activation is exceeded, the immune system must initiate an appropriately balanced immune response that eliminates the pathogen while limiting damage to the lung tissue. Because the lung is not an organized lymphoid tissue, the cellular composition of the lung parenchyma and airways undergoes drastic changes during an immune response (2). Consequently, the lung epithelium is directly exposed to the inflammatory immune response and is therefore susceptible to immune-mediated damage. Thus, failure to tightly regulate the immune response to respiratory pathogens can lead to pulmonary pathology resulting in diminished lung function.

There are multiple regulatory mechanisms in the lungs to control the immune response to respiratory pathogens (1). The initial regulatory barriers in place prior to the induction of an adaptive immune response include active suppression by epithelial cells (3) and alveolar macrophages (4). For instance, exposure of alveolar macrophages to TGF-β that is tethered to airway epithelial cells via the $\alpha_v\beta_6$ integrin serves to maintain macrophages in an anti-inflammatory state and increases the activation threshold of danger signals needed to induce an immune response. Additionally, regulatory Foxp3$^+$ CD4 T cells (Tregs) are essential in regulating the adaptive immune response (5, 6). Identified by expression of the forkhead transcription factor Foxp3 (7, 8), which is required for regulatory function, Foxp3$^+$ Tregs prevent spontaneous inflammation in the lungs (9, 10), control atopic and asthmatic responses (11), and have an important role in establishing mucosal tolerance to Ags (5, 11). In recent years, it has become appreciated that Tregs also play an important role in regulating immune responses to pathogens (12). Most studies examining the role of Tregs during infections have been performed in the context of persistent or chronic infections (13, 14). During chronic infections, Tregs have primarily been shown to limit immunopathology mediated by pathogen-specific T cells and, in some cases, may promote pathogen persistence (15). Importantly, relatively little is known about the role of Tregs during acute virus infections.

To better understand the role of Foxp3$^+$ Tregs during acute respiratory virus infections, we examined the Treg response following acute respiratory syncytial virus (RSV) infection. We show that Foxp3$^+$ Tregs rapidly proliferate and accumulate in the lungs and mediastinal lymph nodes (medLNs) during acute RSV infection. In contrast to Tregs in lymphoid compartments, of which most are CD25$^+$, the frequency of CD25$^+$ Tregs in the lungs is modulated following infection. Additionally, most pulmonary

*Department of Microbiology, †Department of Pathology, and ‡Interdisciplinary Graduate Program in Immunology, University of Iowa, Iowa City, IA 52242

Received for publication February 9, 2010. Accepted for publication June 12, 2010.

This work was supported in part by National Institutes of Health Grant R01 AI063520 (to S.M.V.), Training in Molecular Virology and Viral Pathogenesis Training Grant T32 AI007533, and Training in Mechanisms of Parasitism Training Grant T32 AI007511 (to R.B.F.).

Address correspondence and reprint requests to Dr. Steven Varga, Department of Microbiology, 51 Newton Road, 3-532 Bowen Science Building, University of Iowa, Iowa City, IA 52242. E-mail address: steven-varga@uiowa.edu

The online version of this article contains supplemental material.

Abbreviations used in this paper: aTreg, adaptive Foxp3$^+$ CD4 regulatory T cell; BAL, bronchoalveolar lavage; GITR, glucocorticoid-induced TNFR-related protein; glyco, glycoform; ID, interstitial disease; i.n., intranasal(ly); medLN, mediastinal lymph node; MFI, mean fluorescence intensity; nTreg, natural regulatory T cell; PAS, periodic acid Schiff; PDL, programmed death ligand; Penh, enhanced pause; p.i., postinfection; PVA, perivascular aggregates of leukocytes; RSV, respiratory syncytial virus; Treg, regulatory Foxp3$^+$ CD4 T cell.

www.jimmunol.org/cgi/doi/10.4049/jimmunol.1000423

Tregs upregulate expression of the inhibitory molecule CTLA-4 and acquire an activated phenotype. We demonstrate that Tregs coordinate the early recruitment of virus-specific CD8 T cells into the lung tissue and airways, but they also limit the magnitude of the CD8 T cell response and their ability to produce TNF-α, which likely reduces disease severity. Our data indicate that Tregs play an important role in the regulation of the adaptive CD8 T cell response that is the primary cause of RSV-induced lung immunopathology.

Materials and Methods

Viruses and infection of mice

The A2 strain of RSV was a gift from B.S. Graham (National Institutes of Health, Bethesda, MD) and was propagated on HEp-2 cells (American Type Culture Collection, Manassas, VA). BALB/cAnNCr mice between the ages of 6 and 8 wk were purchased from the National Cancer Institute (Bethesda, MD). Mice were anesthetized with isoflurane and infected with 2–3 $\times$ 10^6 PFU of the A2 strain of RSV intranasally (i.n.). All experimental procedures were approved by the University of Iowa's Animal Care and Use Committee.

Tissue isolation and preparation

The bronchoalveolar lavage (BAL) fluid and lung tissue were harvested from mice as previously described (16). After perfusing the lungs with 5 ml PBS via the right ventricle of the heart, lungs were cut into small pieces and digested in 4 ml HBSS with $CaCl_2$ and $MgCl_2$ (Invitrogen, Grand Island, NY) supplemented with 125 U/ml collagenase (Invitrogen) and 60 U/ml DNase I (Sigma-Aldrich, St. Louis, MO) for 30 min at 37˚C. Lymph nodes were similarly digested in 1 ml HBSS containing collagenase and DNase I as described above. Lungs were then pressed through a wire mesh screen (Cellector; Bellco Glass, Vineland, NJ), and spleens and lymph nodes were pressed between the frosted ends of glass slides (Surgipath, Richmond, IL) to prepare single-cell suspensions.

Cell surface staining

Single-cell suspensions (1×10^6 to 2×10^6 cells) were plated in 96-well round-bottom plates (Corning, Corning, NY) and blocked with anti-FcγRII/III mAb (clone 93) and simultaneously stained with optimal concentrations of mAbs specific for CD4 (clone RM4.5), CD8 (clone 53-6.7), Thy1.2 (clone 53-2.1), CD25 (clone PC61.5), CD45RB (clone C363.16A), CD11a (clone M17/4), CD44 (clone IM7), CD43 (glycosylated; clone 1B11), CD69 (clone H1.2F3), glucocorticoid-induced TNFR-related protein (GITR; clone DTA-1), OX40 (clone OX-86), ICOS (clone 7E.17G9), CD62L (clone MEL-14), CD103 (clone M290), β7 (clone M293), and CD49d (clone R1-2). All mAbs were obtained from eBioscience (San Diego, CA), except for CD43, CD103, and β7, which were obtained from BD Biosciences (San Jose, CA). Cells were stained for 30 min at 4˚C, washed twice with cold staining buffer (PBS, 2% FCS, and 0.02% sodium azide), and subsequently fixed with FACS lysing solution (BD Biosciences). Samples were run on a FACSCanto flow cytometer (BD Biosciences), and data were analyzed using FlowJo software (Tree Star, Ashland, OR).

Tetramer staining

Cells were plated in 96-well round-bottom plates (Corning), washed with staining buffer, and stained with optimal concentrations of RSV $M2_{82–90}$-specific allophycocyanin-conjugated tetramers (obtained from the National Institutes of Health Tetramer Core Facility, Atlanta, GA) and simultaneously blocked with anti-FcγRII/III mAb for 30 min at 4˚C. Cells were washed once with cold staining buffer, stained for cell surface CD8 and Thy1.2, and subsequently washed and fixed with FACS lysing solution prior to analysis by flow cytometry.

Intracellular staining and BrdU

Cells were stained for Foxp3 using a mouse regulatory T cell staining buffer kit (eBioscience) according to the manufacturer's instructions. Briefly, following cell surface staining and fixation, cells were stained with optimal concentrations of mAb specific to Foxp3 (clone FJK-16s; eBioscience), CTLA-4 (clone UC10-4B9; eBioscience), and Ki-67 (clone 35; BD Biosciences). Cells were subsequently washed twice with 1× permeabilization buffer and resuspended in staining buffer. For BrdU studies, mice were administered 2 mg BrdU (Sigma-Aldrich) i.p. and 0.8 mg i.n. in pharmaceutical-grade PBS (Invitrogen) 24 h prior to analysis. To detect BrdU incorporation, cells were first stained for Foxp3 followed by intracellular BrdU staining with mAb specific to BrdU (clone PRB-1; eBioscience) using a BrdU flow kit (BD Biosciences) according to the manufacturers' instructions. DNase I for BrdU staining was obtained from Sigma-Aldrich. Samples were analyzed using flow cytometry.

In vivo depletion of Tregs

Hybridoma cells producing anti-CD25 mAb (clone PC61) were a gift from Thomas Waldschmidt (University of Iowa, Iowa City, Iowa). Anti-CD25 mAb was produced in CELLine CL 1000 chambers (Integra, Hudson, NH) using HyClone SFM4MAb with L-glutamine media (Thermo Fisher Scientific, Waltham, MA) according to the manufacturers' instructions. Anti-CD25 mAb was purified using a 50% ammonium sulfate precipitation and dialyzed with pharmaceutical-grade PBS. To deplete $CD25^+$ CD4 T cells, naive BALB/c mice were administered 1 mg anti-CD25 mAb (PC61) i.p. 3 d prior to infection. Mice were subsequently infected with RSV i.n. and administered 500 μg anti-CD25 mAb i.p. 2 d later. Control mice were administered the same amount of rat IgG (Sigma-Aldrich) in parallel with anti-CD25 mAb treatments. To confirm depletion of $CD25^+$ CD4 T cells, cells were stained for cell surface CD4, Thy1.2, CD25 (clone 7D4; eBioscience), and intracellular Foxp3. The 7D4 clone does not recognize the same epitope on CD25 as does the PC61 mAb used for depletion (17).

Peptide stimulation

Single-cell suspensions derived from the spleen, medLNs, lung, and BAL fluid were plated in 96-well round-bottom plates (Corning) for 5 h at 37˚C with or without 1 μM $M2_{82–90}$ peptide in the presence of 10 μg/ml brefeldin A (Sigma-Aldrich) as previously described (16). Cells were subsequently stained for cell surface CD8 and Thy1.2. After fixation with FACS lysing solution, cells were incubated in permeabilization buffer (staining buffer containing 0.5% saponin; Sigma-Aldrich) for 10 min and stained with optimal concentrations of anti–IFN-γ (clone XMG1.2; eBioscience) and anti–TNF-α (clone MP6-XT22; eBioscience). Cells were washed once with permeabilization buffer and again with staining buffer prior to analysis by flow cytometry.

Measurement of morbidity and airway resistance

Enhanced pause (Penh) was measured using a whole-body plethysmograph (Buxco Electronics, Sharon, CT). Penh values were recorded daily prior to and following infection with RSV. Breathing patterns were recorded for 5 min per mouse to obtain an average Penh value. Mice were weighed daily, and clinical scores were assigned based on the following scale: 0, no apparent illness; 1, slightly ruffled fur; 2, ruffled fur; 3, ruffled fur and inactive; 4, ruffled fur, inactive, hunched posture; and 5, moribund or dead.

Plaque assays

Lungs were harvested from RSV-infected mice on days 4, 6, and 7 postinfection (p.i.) and processed for plaque assays on Vero cells as previously described (18).

Histology

Whole lungs with the heart attached were removed from control or Treg-depleted mice 7 d p.i. Lungs were placed in 10% formalin (Thermo Fisher Scientific) in a vacuum to remove air from the lungs. Fixed lungs were embedded in paraffin, sectioned at 4-μm thickness, and either H&E or periodic acid Schiff (PAS) stained by the University of Iowa Comparative Pathology Laboratory. Slides were blinded and scored by a board-certified veterinary pathologist (D. Meyerholz, University of Iowa). Stained sections were scored for perivascular aggregates of leukocytes from 1 to 4 on a graded scale in which 1 represents normal parameters and 4 represents moderate to high cellularity. Interstitial disease was scored on the following scale: 1, within normal parameters; 2, mild, detectable focal to multifocal congestion, uncommon to small numbers of leukocytes and some atelectasis; 3, moderate, multifocal to coalescing congestion, leukocyte cellularity, and atelectasis with rare luminal leakage of cellular and fluid debris; and 4, severe, coalescing interstitial congestion, leukocytes, and atelectasis with admixed extensive loss of airspace and luminal accumulation of cellular and fluid debris. Edema was scored from 1 to 4 on a graded scale in which 1 represents no edema and 4 represents multiple fields having coalescing alveoli filled by pools of fluid. Mucus airway obstruction was scored on the following scale: 1, normal epithelium and no luminal accumulation; 2, epithelial mucinous hyperplasia with thin strands of mucus lining the airways; 3, epithelial mucinous hyperplasia with luminal mucus accumulation partially filling the airways; and 4, epithelial mucinous hyperplasia with luminal mucus filling and obstructing the airways.

Data analysis

Graphical analysis was performed using Prism software (Graphpad Software, San Diego, CA). Statistical analyses were performed using InStat

software (Graphpad Software). Comparisons between two groups with normal Gaussian distributions were analyzed using paired or unpaired *t* tests (two-tailed), a Welch corrected unpaired *t* test for data with significant differences in SD between groups, or a Mann-Whitney *U* test for data without Gaussian distributions. Within-group comparisons to baseline were analyzed using a one-way ANOVA with a Dunnett posttest to control for multiple comparisons. Overall trends in longitudinal data between groups were analyzed using two-way repeated-measures ANOVA. The $p < 0.05$ values were considered significant.

Results

Foxp3$^+$ Tregs rapidly accumulate in the lungs and medLNs during RSV infection

Treg responses to pathogens have been extensively studied in the context of persistent or chronic infections (13–15, 19, 20). In contrast, much less is known concerning the role of Tregs during acute infections (21). Following acute infection of BALB/c mice with RSV, the frequency of CD4 T cells that were Foxp3$^+$ increased in the lung airways (BAL), lung parenchyma, and lung-draining medLNs (Fig. 1*A*–*C*). By day 4 p.i., 25% of CD4 T cells in the BAL were Foxp3$^+$, representing an ~50-fold increase in absolute numbers over naive levels (Fig. 1*A*). By day 8 p.i., the total number of Tregs in the BAL had increased 86-fold over naive levels. The lung parenchyma also exhibited an increase in the frequency and total number of Tregs (Fig. 1*B*). By day 6 p.i. the frequency of CD4 T cells that were Foxp3$^+$ more than doubled compared with naive levels (17% compared with 7%), which represented an ~3-fold increase in total numbers of Tregs over naive levels. Thus, following infection with RSV there was an early enrichment of Tregs in the BAL and lung parenchyma. In contrast, the frequency of Foxp3$^+$ CD4 T cells in the medLNs remained relatively constant except for an early increase on day 2 p.i. (Fig. 1*C*). However, the absolute number of Tregs rapidly increased during the first several days p.i., indicating that the accumulation of Tregs paralleled that of Foxp3$^-$ CD4 T cells (data not shown). In contrast to the lungs and medLNs, we did not observe large fluctuations in the frequency or total number of Foxp3$^+$ CD4 T cells in the spleen or PBLs (Fig. 1*D*, 1*E*).

Concomitant with clearance of RSV from the lungs by day 7 p.i (22), the number of Tregs decreased in the BAL, lung parenchyma, medLNs, and spleen (Fig. 1*A*–*D*). By day 15 p.i., the absolute number of Tregs in the lung parenchyma and spleen had nearly returned to baseline levels. The decline in Treg numbers was more prolonged in the BAL and medLNs, but total numbers were similar to baseline levels at day 220 p.i. We observed an increase in the frequency of Foxp3$^+$ CD4 T cells in the medLNs and spleen by day 220 p.i. along with increased Treg numbers in the spleen (Fig. 1*C*, 1*D*), which is consistent with studies showing an increase in Foxp3$^+$ Tregs in mice as they age (15, 23). The kinetics of the Treg response to RSV infection was not unique to BALB/c mice; we observed similar kinetics in the BAL, lung parenchyma, medLNs, spleen, and PBLs following acute RSV infection of C57BL/6 Foxp3^{gfp} mice (data not shown).

Proliferation of Foxp3$^+$ Tregs during RSV infection

The accumulation of Foxp3$^+$ Tregs in the medLNs and lungs during RSV infection could be explained by the recruitment and/or proliferation of Tregs. To determine whether Tregs proliferate in response to RSV infection, we examined BrdU incorporation in parallel with the proliferation marker Ki-67. Twenty-four hours prior to analysis, naive or RSV-infected BALB/c mice were administered BrdU both i.p. and i.n. to ensure efficient incorporation of BrdU by proliferating cells in the lung parenchyma and BAL (24). Consistent with previous reports (11, 25, 26), prior to infection the percentage of Tregs that were Ki-67$^+$ or BrdU$^+$ was significantly higher than conventional Foxp3$^-$ CD4 T cells ($p < 0.01$ for all except Ki-67 frequencies in the BAL) (Fig. 2). Following RSV infection, there was an increase in the

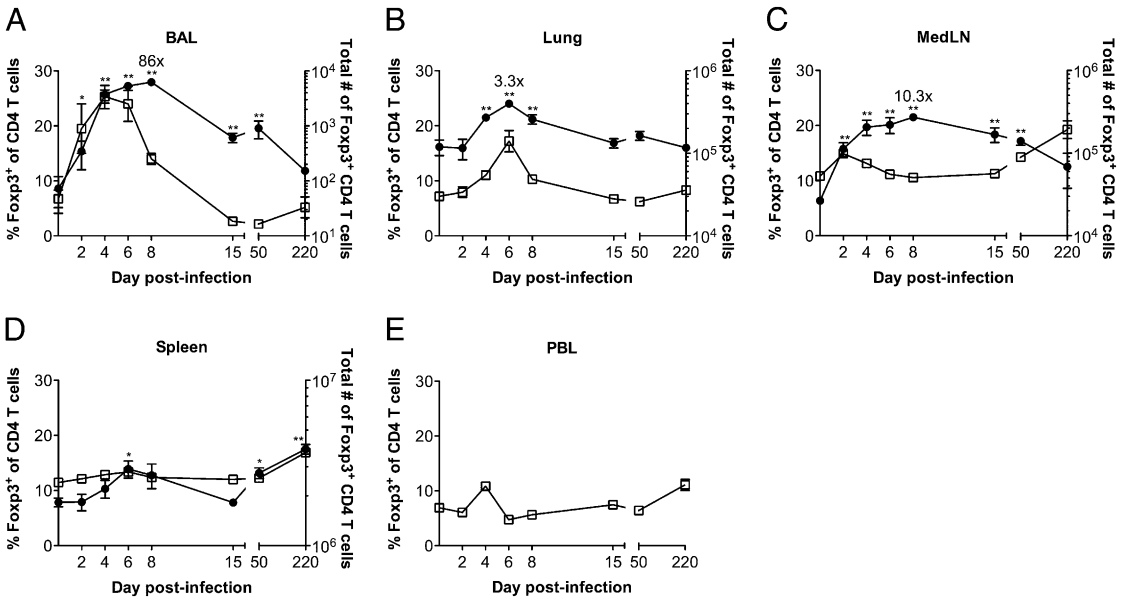

FIGURE 1. Foxp3$^+$ Tregs accumulate in the lungs and medLNs following RSV infection. BALB/c mice were infected with RSV i.n., and cells from the BAL (*A*), lung parenchyma (*B*), medLNs (*C*), spleen (*D*), and PBLs (*E*) were collected at the indicated times. The percentage of CD4 T cells that are Foxp3$^+$ (open squares, *left y-axis*) and the total number of Foxp3$^+$ CD4 T cells (filled circles, *right y-axis*) were determined by flow cytometry. In *E*, only the percentage of CD4 T cells that are Foxp3$^+$ is shown. Numbers in the plots represent the fold increase in the total number of Foxp3$^+$ Tregs over naive controls. The data for the spleen, medLNs, and PBLs represent the mean ± SEM from two separate experiments at each time point with four mice per experiment, except for day 50, which represents three separate experiments. Data for the lung parenchyma and BAL represent data from two separate experiments on days 2, 8, 15, and 220; three experiments on days 0, 4, and 50; and four experiments on day 6. BAL was pooled from four mice per experiment and divided by four to determine the total number of cells. Statistical analysis of total numbers of Tregs compared with baseline (day 0) numbers was done on $\log_{10}$-transformed data using one-way ANOVA with Dunnett posttests. $*p < 0.05$; $**p < 0.01$.

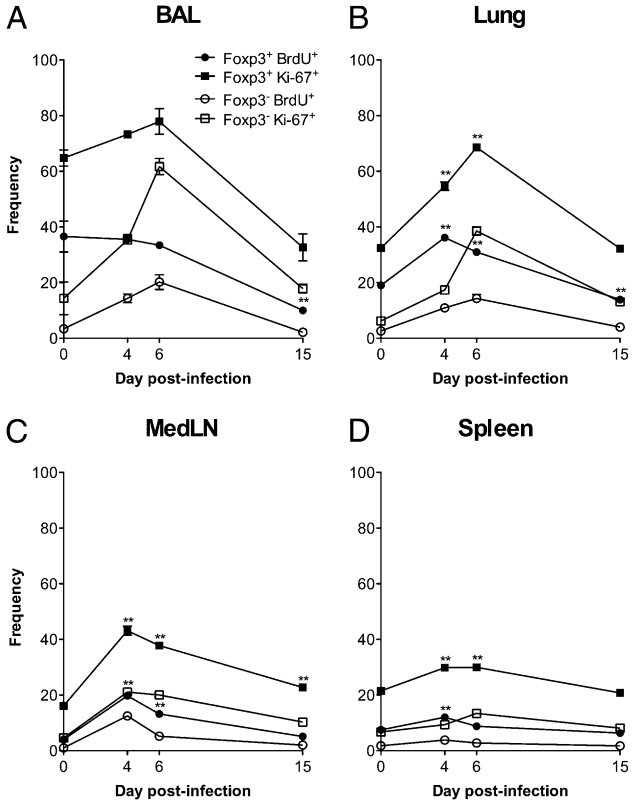

FIGURE 2. Foxp3$^+$ Tregs proliferate in response to RSV infection. Naive or RSV-infected BALB/c mice were administered BrdU i.p. and i.n., and cells were harvested 24 h later at the times indicated. The percentages of Foxp3$^-$ (open symbols) or Foxp3$^+$ (filled symbols) CD4 T cells that were BrdU$^+$ (circles) or Ki-67$^+$ (squares) are shown for Tregs from the BAL (*A*), lung parenchyma (*B*), medLNs (*C*), and spleen (*D*). Data represent the mean ± SEM from four separate experiments for BrdU data and two separate experiments for Ki-67 data at each time point with four mice per experiment. BAL was pooled from four mice per experiment. Statistical analysis of the frequencies of BrdU$^+$ or Ki-67$^+$ Foxp3$^+$ Tregs compared with baseline levels (day 0) was done using one-way ANOVA with Dunnett posttests. $^{**}p < 0.01$.

frequency of proliferating Tregs in the BAL, lung parenchyma, medLNs, and spleen compared with naive controls. By day 6 p.i., 78% and 69% of Tregs in the BAL and lung parenchyma, respectively, were Ki-67$^+$. In the spleen there was a much smaller increase over naive levels relative to the lungs and medLNs (Fig. 2*D*). By day 15 p.i. the frequency of proliferating Tregs in the lungs, medLNs, and spleen had decreased to levels comparable to naive mice. Due to the relatively short 24-h BrdU pulse, we consistently observed higher frequencies of Ki-67$^+$ compared with BrdU$^+$ CD4 T cells. Interestingly, we observed a higher percentage of Foxp3$^+$ Tregs undergoing proliferation as compared with Foxp3$^-$ CD4 T cells at all times examined. These results demonstrate that RSV infection induces local proliferation of Tregs, which contributes to the accumulation of Foxp3$^+$ Tregs in the BAL, lung parenchyma, and medLNs.

CD25 expression by Foxp3$^+$ Tregs during RSV infection

Because Tregs were proliferating and presumably becoming activated in response to RSV infection, we next wanted to examine the phenotype of pulmonary Tregs following infection. Although IL-2 is essential for the peripheral maintenance of Tregs (27, 28), it has previously been shown that whereas most Foxp3$^+$ CD4 T cells are CD25$^+$ in secondary lymphoid tissues, this frequency is decreased in the lungs (29). To determine whether CD25 was modulated during the course of infection, we tracked CD25 expression by Foxp3$^+$ Tregs (Fig. 3). The frequencies of CD25$^+$ Foxp3$^+$ Tregs in the medLNs and spleen remained relatively stable at ~80% throughout the course of infection (Fig. 3). As expected, in naive mice 59% of Tregs in the lung parenchyma were CD25$^+$. In contrast, 74% of Tregs in the BAL of naive mice were CD25$^+$, suggesting that Tregs in the lung airways may upregulate CD25 expression or that CD25$^+$ Tregs are preferentially recruited to, or retained in, the airways. Following infection, the percentage of CD25$^+$ Tregs in the lung parenchyma dipped to 50% and remained relatively stable afterward. In contrast to the lung parenchyma, ~70–75% of Tregs in the BAL remained CD25$^+$ during the first 8 d of infection. The frequency then decreased to 54% by day 15 p.i. before eventually returning to baseline levels by day 220.

Pulmonary Tregs acquire an activated phenotype during RSV infection

To further assess the activation phenotype of Tregs, we compared pulmonary Tregs from naive or RSV-infected mice for markers commonly associated with T cell activation. Consistent with previous reports that Tregs from naive mice display an effector cell phenotype (17, 30), >90% of pulmonary Tregs were CD45RB^{low} and ~40% were high for the memory markers CD11a and CD44 (Fig. 4). Approximately 40% of Tregs expressed the activation-associated glycoform (glyco) of CD43 (CD43^{glyco}) and the costimulatory receptor ICOS, suggesting that some Tregs may have been recently activated. A low frequency (<4%) of Tregs expressed CD69 and OX40, and >90% were GITR^{high} and FR4^{high} (Supplemental Fig. 1). CTLA-4 is an inhibitory homolog of CD28 that is constitutively expressed by a portion of Tregs and has been implicated as a regulatory mechanism used by Tregs (9, 31–33). In the lung parenchyma, 37% of Tregs were CTLA-4$^+$. Few Tregs expressed the inhibitory molecules LAG-3, programmed death 1, or programmed death ligand (PDL)-2 (data not shown). However, 15% of Foxp3$^+$ Tregs expressed PDL-1 (Supplemental Fig. 1).

By day 6 p.i., pulmonary Tregs further downregulated CD45RB expression, 70–80% became CD11a^{high} and CD44^{high}, and there was an ~2.5-fold increase in the geometric mean fluorescence intensity (MFI) of GITR compared with Tregs from the lung parenchyma of naive mice (Fig. 4, data not shown). We also observed a significant ($p < 0.01$) increase in the frequency of Tregs expressing CD43^{glyco} (70%), ICOS (81%), CTLA-4 (78%), CD69 (34%), OX40 (21%), and PDL-1 (62%) compared with Tregs from the lungs of naive mice (Fig. 4, Supplemental Fig. 1). There were minimal changes in LAG-3, programmed death 1, and PDL-2 expression (data not shown). These data further demonstrate that pulmonary Tregs are highly activated during acute RSV infection.

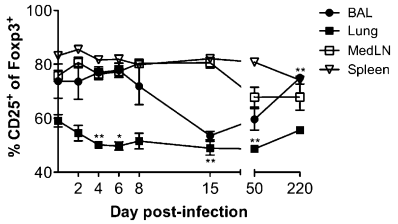

FIGURE 3. Foxp3$^+$ Tregs modulate CD25 expression following RSV infection. BALB/c mice were infected with RSV i.n., and the percentages of Foxp3$^+$ Tregs expressing CD25 in the BAL, lung parenchyma, medLNs, and spleen were determined at the times indicated. Data represent the mean ± SEM from two to three separate experiments except for data from day 220, which represents a single experiment. There were four mice per experiment at each time point. BAL was pooled from four mice per experiment. Statistical analysis of the frequencies of CD25$^+$ Tregs compared with baseline levels (day 0) was done using one-way ANOVA with Dunnett posttests. $^{*}p < 0.05$; $^{**}p < 0.01$.

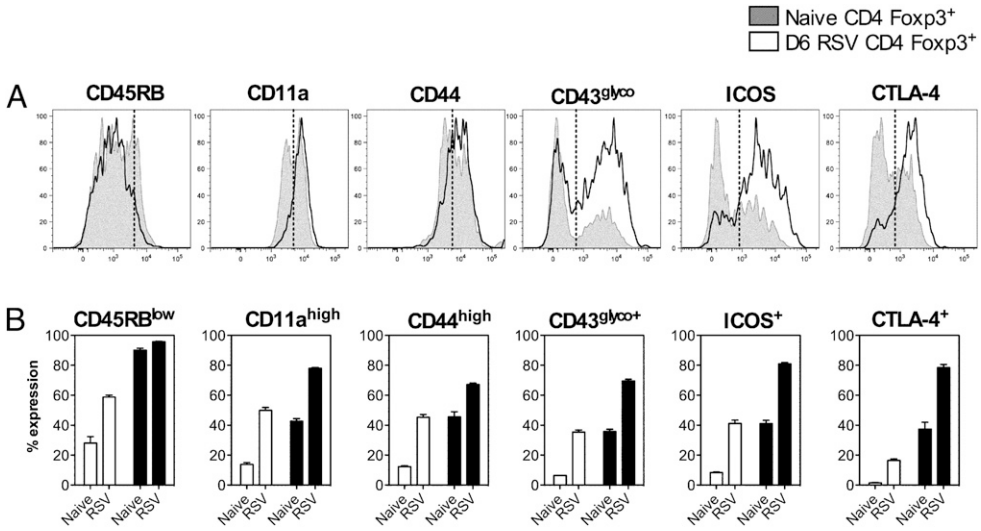

FIGURE 4. Pulmonary Tregs acquire an activated phenotype following RSV infection. Cells from the lung parenchyma (post-BAL) were stained for various markers and intracellular Foxp3. *A*, Histogram plots are gated on Foxp3$^+$ CD4 T cells from naive mice (gray shaded) or from mice infected with RSV 6 d earlier (solid line). Vertical dotted lines indicate where gates were drawn based on isotype staining (CD43^{glyco}, ICOS, and CTLA-4) or for CD45RB, CD11a, and CD44 expression. CD43^{glyco} is the activation-associated glycoform of CD43. Plots are representative of data from two separate experiments. *B*, Cumulative data from histograms showing marker expression by Foxp3$^-$ (□) and Foxp3$^+$ (■) CD4 T cells from the lungs of naive or RSV-infected lungs 6 d p.i. Error bars represent the SEM. Data were analyzed using Welch corrected unpaired *t* tests. Relative to naive mice within each subset (Foxp3$^-$ or Foxp3$^+$), all changes in percent expression of markers in RSV-infected mice were statistically significant. $p < 0.01$.

Pulmonary Tregs modulate trafficking molecules during infection

We also examined the modulation of trafficking molecules on pulmonary Tregs. In naive mice, 23% of pulmonary Tregs had low expression of CD62L (Fig. 5). By day 6 p.i., 54% of Tregs in the lung parenchyma had low CD62L expression. The $\alpha_E\beta_7$ integrin has been shown to be important for Treg trafficking to sites of inflammation, such as the skin and lungs (30, 34). The frequency of α_E- and β_7-expressing Tregs in the lung parenchyma increased from 30% and 45%, respectively, in naive mice to 40% and 67%, respectively, by day 6 p.i. (Fig. 5). When compared with Foxp3$^-$ CD4 T cells, expression of the α_E and β_7 integrin chains were primary restricted to Foxp3$^+$ CD4 T cells, suggesting that $\alpha_E\beta_7$ integrin may be important for Treg trafficking into the lungs during RSV infection. Additionally, the $\alpha_4\beta_1$ integrin (VLA-4) has been demonstrated to be important for trafficking of lymphocytes into BALT via VCAM-1 expressed on high endothelial venules (35). We observed an increase in the frequency of both Foxp3$^+$ Tregs and Foxp3$^-$ CD4 T cells expressing high levels of the α_4 integrin chain. Thus, the α_4 integrin chain may also be important in trafficking of both Treg and effector CD4 T cells into the lungs.

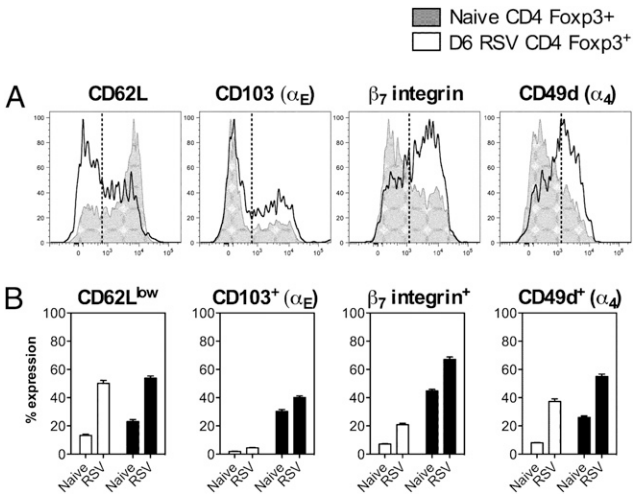

FIGURE 5. Pulmonary Tregs modulate trafficking molecules following RSV infection. Cells from the lung parenchyma (post-BAL) were stained for various extracellular markers and intracellular Foxp3. *A*, Histogram plots are gated on Foxp3$^+$ CD4 T cells from naive mice (gray shaded) or from mice infected with RSV 6 d earlier (solid line). Vertical dotted lines indicate where gates were drawn based on isotype staining (CD62L and CD103) or for β7 and CD49d expression. Plots are representative of data from two separate experiments. *B*, Cumulative data from histograms showing marker expression by Foxp3$^-$ (□) and Foxp3$^+$ (■) CD4 T cells from the lungs of naive or RSV-infected lungs 6 d p.i. Error bars represent the SEM. Data were analyzed using Welch corrected unpaired *t* tests. Relative to naive mice within each subset (Foxp3$^-$ or Foxp3$^+$), all changes in percentage expression of markers in RSV-infected mice were statistically significant. $p < 0.01$.

Depletion of Tregs delays virus clearance

Depletion of Tregs has been shown in most infection models to accelerate pathogen clearance due to enhanced T cell responses (13–15, 36). Therefore, we next determined whether depletion of Tregs altered the rate of virus clearance in the lungs. Naive mice were treated with anti-CD25 mAb 3 d prior to RSV infection and a second time 2 d p.i. to ensure sustained depletion of CD25$^+$ Tregs. At the time of infection, in the lung parenchyma there was an ~86% reduction in the percentage of Foxp3$^+$ Tregs that were CD25$^+$ as detected by the anti-CD25 mAb clone 7D4 (Supplemental Fig. 2*A*). This decrease corresponded with an ~60% reduction in the frequency of Foxp3$^+$ CD4 T cells, consistent with the depletion of this population (Supplemental Fig. 2*B*). The residual frequency of Foxp3$^+$ Tregs was expected based on our previous observation that only 59% of Tregs in the lung express CD25 (Fig. 3). There were similar virus titers on days 4 and 6 p.i. in the lungs of control and Treg-depleted mice (Fig. 6). However, despite only being able to eliminate 60% of the Tregs in the lung via anti–CD25-mediated depletion, we observed a significant ($p < 0.01$) delay in virus clearance (Fig. 6). These data suggest that the virus-specific CD8 T cell response, which is necessary to

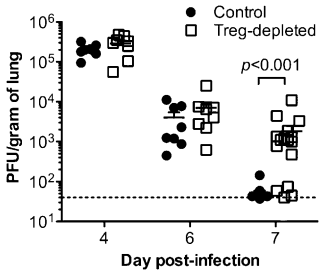

FIGURE 6. Depletion of Tregs delays virus clearance. Tregs were depleted in BALB/c mice with anti-CD25 mAb (clone PC61) treatment as described in *Materials and Methods*. Control mice received rat IgG. Following infection with RSV, virus titers were measured in the lungs of control or Treg-depleted mice. The dashed line represents the limit of detection. Data represent two separate experiments for days 4 and 6 p.i. and four separate experiments for day 7 p.i. with four mice per experiment. Error bars represent the SEM. Data were analyzed using nonparametric Mann-Whitney *U* tests.

mediate clearance of RSV (37, 38), might be negatively affected when Treg numbers are reduced during infection.

Depletion of CD25$^+$ Tregs delays the recruitment of RSV-specific CD8 T cells into the lung

Multiple studies have shown that Tregs limit the magnitude of pathogen-specific CD8 T cell responses (13, 21, 39, 40), which would appear to be at odds with our data demonstrating that virus clearance is delayed in Treg-depleted mice. Therefore, we next sought to examine the impact of Treg depletion on the magnitude and kinetics of the RSV-specific CD8 T cell response. Consistent with the role of Tregs in limiting overall inflammation, there were significantly ($p < 0.01$) more total cells in the lung parenchyma of Treg-depleted mice at both days 6 and 8 p.i. (Fig. 7*A*). Total cell numbers in the BAL and medLNs were similar between groups on both days examined. On days 6 and 8 p.i. there were increased numbers of CD4 T cells in the lung parenchyma, and on day 8 p.i. there were more CD8 T cells in the lung parenchyma and medLNs (Fig. 7*B*, 7*C*). There were also substantially more NK cells (CD3$^-$DX5$^+$) 6 d p.i. and more B cells (CD19$^+$B220$^+$) and neutrophils (Ly6C$^+$Ly6G$^+$CD11b$^+$) 8 d p.i. in the lung parenchyma of Treg-depleted mice (Fig. 7*D*).

To determine the effect of Treg depletion on the RSV-specific CD8 T cell response, we enumerated Ag-experienced CD11a^{high}CD44^{high} CD8 T cells in the medLNs, lung parenchyma, and BAL (Fig. 8*A*) (41). In Treg-depleted mice there were significantly ($p < 0.01$) more CD11a^{high}CD44^{high} CD8 T cells in the medLNs on days 6 and 8 p.i. In contrast, there were significantly ($p < 0.05$) fewer CD11a^{high}CD44^{high} CD8 T cells in the lung parenchyma on day 6 p.i. However, by day 8 there was an ~1.6-fold increase in the number of Ag-experienced CD8 T cells compared with control mice. This increase was reflective of the ~1.6-fold increase in total CD8 T cells (Fig. 7*C*). There was no statistical difference observed in the BAL between control and Treg-depleted mice.

We next examined the immunodominant $M2_{82–90}$ CD8 T cell response. On day 6 p.i. there were similar frequencies and numbers of $M2_{82–90}$ tetramer-specific CD8 T cells in the medLNs of Treg-depleted mice compared with controls (Fig. 8*B*). However, following ex vivo $M2_{82–90}$ peptide stimulation, we observed a higher percentage of IFN-γ^+ CD8 T cells in the medLNs of Treg-depleted mice (4.4 ± 0.3% in IgG-treated compared with 6.6 ± 0.6% in PC61-treated mice; $p < 0.01$) at day 6 p.i. The discrepancy in frequencies of $M2_{82–90}$-specific CD8 T cells in the medLNs at day 6 p.i. as measured by tetramer or IFN-γ is likely a result of decreased tetramer binding to newly activated T cells due to rearrangement of surface TCRs (42). As indicated by the decrease in CD11a^{high}CD44^{high} CD8 T cells, there was a significant ($p < 0.01$) decrease in both the frequency and total number of $M2_{82–90}$ tetramer-specific CD8 T cells in the lung parenchyma of Treg-depleted mice at day 6 p.i. (Fig. 8*B*). We observed similar differences in the lung parenchyma and BAL in the percentage of IFN-γ^+ CD8 T cells following ex vivo peptide stimulation (data not shown). These data suggest that there is impaired egress of $M2_{82–90}$-specific CD8 T cells from the

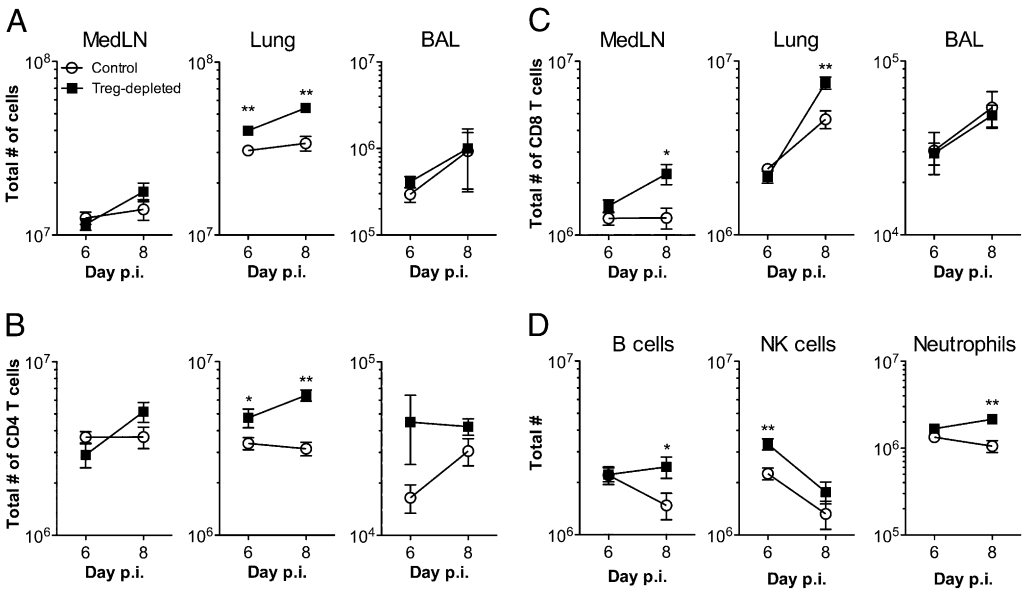

FIGURE 7. Total numbers of cells in the medLNs, lung parenchyma, and BAL of control or Treg-depleted mice. BALB/c mice were depleted of Tregs prior to acute RSV infection. Total numbers of cells (*A*), CD4 T cells (*B*), and CD8 T cells (*C*) in the medLNs, lung parenchyma, and BAL were determined in control or Treg-depleted mice on days 6 and 8 p.i. *D*, Total numbers of B cells (CD19$^+$B220$^+$), NK cells (CD3$^-$DX5$^+$), and neutrophils (Ly6C$^+$Ly6G$^+$CD11b$^+$) were enumerated by flow cytometry in the lungs (post-BAL) 6 and 8 d p.i. Data in *A* and *C* represent five experiments on day 6 p.i. and two experiments on day 8 p.i. with four mice per experiment. Data in *B* and *D* represent two experiments with four mice per experiment. Error bars represent the SEM. All data were $\log_{10}$-transformed prior to statistical analysis with unpaired *t* tests. $*p < 0.05$; $**p < 0.01$.

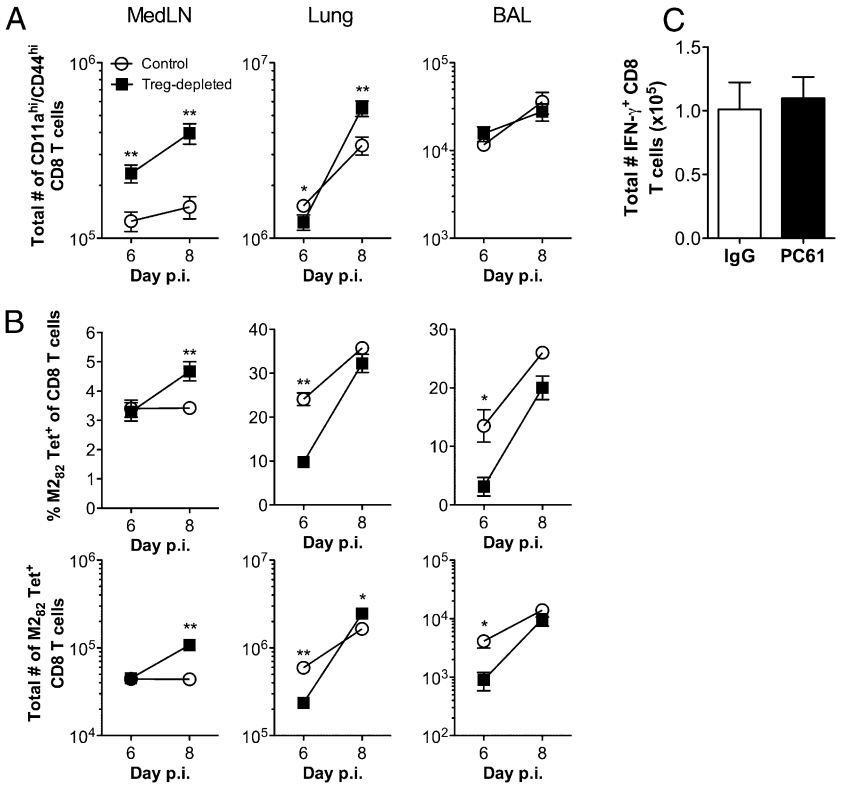

FIGURE 8. Decreased early recruitment of RSV-specific CD8 T cells into the lungs in Treg-depleted mice. BALB/c mice were depleted of Tregs prior to acute RSV infection. *A*, Total numbers of $CD11a^{high}CD44^{high}$ CD8 T cells were determined in the medLNs, lung parenchyma, and BAL 6 and 8 d p.i. Cells from the medLNs and lung parenchyma of naive mice were used to determine the gating for $CD11a^{high}CD44^{high}$ CD8 T cells in RSV-infected mice. Data represent five experiments on day 6 p.i. and two experiments on day 8 p.i. with four mice per experiment. *B*, Frequency (*top*) and total numbers (*bottom*) of $M2_{82–90}$ tetramer$^+$ CD8 T cells in the medLNs, lung parenchyma, and BAL 6 and 8 d p.i. MedLNs and lungs from naive mice were used as controls for tetramer staining. Data represent three experiments on day 6 p.i. and two experiments on day 8 p.i. with four mice per experiment. *C*, Total numbers of IFN-γ^+ $M2_{82–90}$-specific CD8 T cells in the spleen 6 d p.i. Data represent two experiments with four mice per experiment. Error bars represent the SEM. Data were analyzed using unpaired *t* tests. Data were $\log_{10}$-transformed except for the *top panel* of *B* prior to analysis. $*p < 0.05$; $**p < 0.01$.

lung-draining LNs into the lungs. Importantly, these data argue against the possibility of nonspecific depletion of activated CD8 T cells that have upregulated CD25 expression as the cause of the decrease in the $M2_{82–90}$-specific CD8 T cell response in the lungs. Furthermore, we observed similar frequencies and total numbers of $M2_{82–90}$-specific IFN-γ^+ CD8 T cells in the spleen at day 6 p.i. (Fig. 8*C*, data not shown). By day 8 p.i. in Treg-depleted mice, total numbers of $M2_{82–90}$ tetramer-specific CD8 T cells were similar to (BAL) or exceeding (lung parenchyma and medLNs) those of control mice, which is in agreement with evidence that Tregs limit the magnitude of the CD8 T cell response (21, 39, 40). These data suggest that Tregs are important in coordinating early trafficking of virus-specific CD8 T cells into the lung parenchyma and airways.

Tregs limit disease severity during RSV infection

Given the altered kinetics of CD8 T cell accumulation in the lung, we next assessed morbidity in Treg-depleted mice. When compared with control mice, Treg-depleted mice exhibited increased clinical illness on days 7 and 8 p.i. (Fig. 9*A*), which was accompanied by increased weight loss (Fig. 9*B*). We used whole-body plethysmography to determine whether depletion of Tregs resulted in increased Penh during RSV infection (Fig. 9*C*). Mice depleted of Tregs exhibited a delayed rise in Penh compared with control mice. Increased Penh values were sustained in Treg-depleted mice, which could not be simply accounted for by a single day delay (day 8 Treg-depleted versus day 7 control, $p = 0.002$; day 9 Treg-depleted versus day 8 control, $p = 0.02$). These data indicated that depletion of Tregs results in increased airway resistance during infection. Lungs from Treg-depleted mice had increased severity of perivascular aggregates of leukocytes that primarily consisted of lymphocytes (Fig. 10). When compared with control mice, the lung airways of Treg-depleted mice also had more severe epithelial mucinous hyperplasia with luminal mucus filling and obstructing the airways. Thus, Treg depletion results in increased disease during the late immune phase that coincides with the adaptive immune response.

Depletion of Tregs enhances TNF-α production by CD8 T cells

The exacerbated disease severity observed in Treg-depleted mice during RSV infection could be explained by delayed virus clearance and/or enhanced T cell-mediated immunopathology. In Treg-depleted mice, CD8 T cells could contribute to enhanced disease by producing increased amounts of the proinflammatory cytokine TNF-α. TNF-α has been shown to be a major cause of illness during acute RSV infection (43). Following ex vivo peptide stimulation, higher frequencies of $M2_{82–90}$-specific CD8 T cells from Treg-depleted mice were capable of coproducing IFN-γ and TNF-α relative to control mice (Fig. 11*A*, 11*B*). When compared with control mice, a higher frequency of CD8 T cells isolated from the lung parenchyma and BAL of Treg-depleted mice coproduced IFN-γ and TNF-α on day 6 p.i. and from the medLNs on both 6 and 8 d p.i. The MFI of TNF-α in Treg-depleted mice was substantially higher than in control mice; there was an ~1.5-fold and an ~1.9-fold increase in the TNF-α MFI in the lung parenchyma and BAL, respectively, on day 6 p.i. (Fig. 11*A*, 11*C*). In the medLNs there was an ~1.7-fold increase in TNF-α MFI on both 6 and 8 d p.i. Consequently, increased in vivo production of TNF-α in Treg-depleted mice would likely contribute to enhanced disease.

Discussion

Most studies examining Foxp3$^+$ Tregs during immune responses to pathogens have focused on pathogens that establish chronic infections (13, 14). Because depletion of Tregs prior to acute infection with lymphocytic choriomeningitis virus, the most widely studied virus in viral immunology, did not appear to affect the CD8 T cell response (13), much of the focus has remained on chronic infection models. Regardless of the reasons, much less is known about the Treg response to pathogens during acute infections.

To characterize the activation state of Tregs during acute RSV infection, we examined a broad panel of T cell activation markers. Given that IL-2 is crucial for the maintenance of Tregs in the

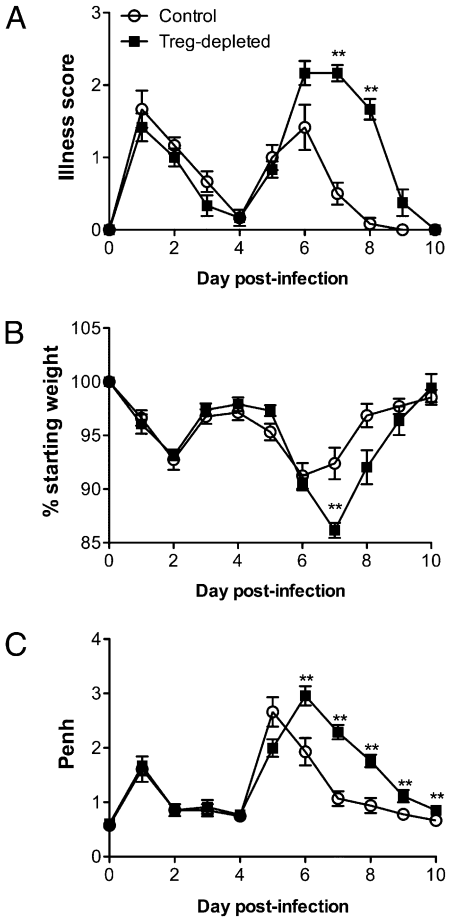

FIGURE 9. Depletion of Tregs exacerbates the severity of RSV-induced disease. BALB/c mice were depleted of Tregs prior to acute RSV infection. Mice were monitored daily for clinical illness (*A*), weight loss (*B*), and airway resistance (Penh) (*C*). Airway resistance was assessed using a whole-body plethysmograph. Data represent the mean ± SEM from three separate experiments with four mice per experiment. Statistical analysis found a difference in weight loss and Penh in the overall trends between control and Treg-depleted mice using two-way repeated-measures ANOVA. $p = 0.0001$; $p < 0.0001$, respectively. Individual days in *A–C* were analyzed using nonparametric Mann-Whitney *U* tests. $^{**}p < 0.01$.

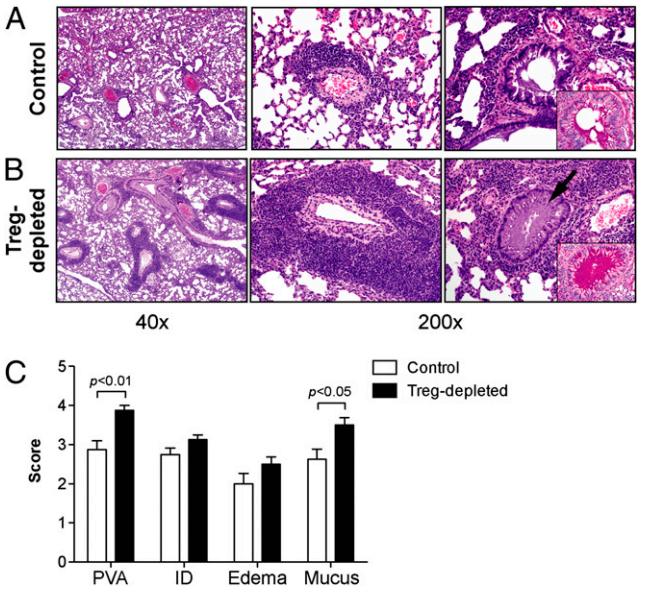

FIGURE 10. Increased inflammation and mucus in the lungs of Treg-depleted mice. Whole lungs from control (*A*) or Treg-depleted mice (*B*) were collected, sectioned, and either H&E or PAS stained. Sections were scored for perivascular aggregates of leukocytes, interstitial disease, edema, and mucus. On low magnification (original magnification ×40), control and Treg-depleted mice were distinguished by prominent perivascular inflammation (*left panels*) that was mostly composed of lymphoid cells (*middle panels*, original magnification ×200). Treg-depleted mice also had severe mucinous changes (*right panels*, original magnification ×200) with some airways completely obstructed by mucus (arrow). *Insets* in the *right panels* are PAS-stained serial sections that highlight magenta stained mucus in the airway lumen (original magnification ×400). *C*, Cumulative histological scores. Images (*A*, *B*) and scores (*C*) are representative of eight mice per group. All data were analyzed using nonparametric Mann-Whitney *U* tests. ID, interstitial disease; PVA, perivascular aggregates of leukocytes.

periphery (27), it is curious that roughly half of Foxp3$^+$ Tregs in the lungs do not express CD25. The high-affinity IL-2R is composed of CD25 (IL-2Rα), CD122 (IL-2Rβ), and CD132 (common γ-chain). Although IL-2 can still signal through the low-affinity IL-2R composed of the IL-2Rβ and common γ-chains, the low-affinity IL-2R is not sufficient for peripheral Treg maintenance, as IL-2– or CD25-deficient mice have a drastic reduction in the frequency of peripheral Tregs and suffer from severe autoimmunity (27, 28). After IL-2 binds the IL-2R, the complex is internalized and CD25 is recycled back to the cell surface. Because ~20% of Foxp3$^+$ Tregs do not express CD25 at any given time, this may reflect a population of Tregs that recently bound IL-2. Thus, the high frequency of Tregs in the lung that do not express CD25 may reflect cells that recently received IL-2 signals.

Additional analysis of activation-associated molecules on Tregs during infection revealed that the vast majority of Tregs in the lungs exhibited an activated phenotype (CD11a^{high}, CD44^{high}, CD43^{glyco+}, ICOS$^+$, CTLA-4$^+$) and had upregulated expression of the α_4 and β_7 integrin chains. Relative to the Foxp3$^+$ Treg population, the frequency of Foxp3$^-$ CD4 T cells expressing these molecules was notably reduced. This is perhaps not unexpected since the conventional CD4 T cell response is likely made up of a diverse array of differentiated subsets and memory CD4 T cells nonspecifically recruited into the lung. However, it has been suggested that some of the markers expressed by Tregs identify distinct populations with different inhibitory mechanisms or trafficking profiles. For instance, it has been suggested that expression of the α_E integrin chain or the costimulatory receptor ICOS may identify two functionally distinct subsets of Foxp3$^+$ Tregs (30, 34, 44–46). Following RSV infection, most Tregs in the lung parenchyma and BAL (data not shown) upregulated CTLA-4. Recent studies have shown that CTLA-4 expressed by Foxp3$^+$ Tregs is required to maintain systemic tolerance (9, 31). However, in the context of an infection, it is unknown whether Treg-specific expression of CTLA-4 is required to regulate T cell activation or whether CTLA-4 expressed by nonregulatory T cells is sufficient. Because effector T cells also express CTLA-4 during infection, it is less clear to what extent CTLA-4 expressed by Tregs regulates T cell activation and proliferation. Further studies using CTLA-4 conditional knockout mice lacking CTLA-4 in Foxp3$^+$ Tregs would help to elucidate the role of Treg-associated CTLA-4 during RSV infection.

Although our data revealed that Tregs are activated during RSV infection, it is not clear what signals induce the activation of Tregs. This is especially unclear for natural Tregs (nTregs), which are thought to recognize self-Ags (14, 47). If one assumes that most of the Foxp3$^+$ Tregs responding to RSV infection are nTregs, there are several possible ways to explain their activation (13). One possibility is that nTregs recognize tissue-specific Ags in the context of nontolerogenic inflammation caused by the infection. Another possibility is that nTregs recognize pathogen-derived Ags.

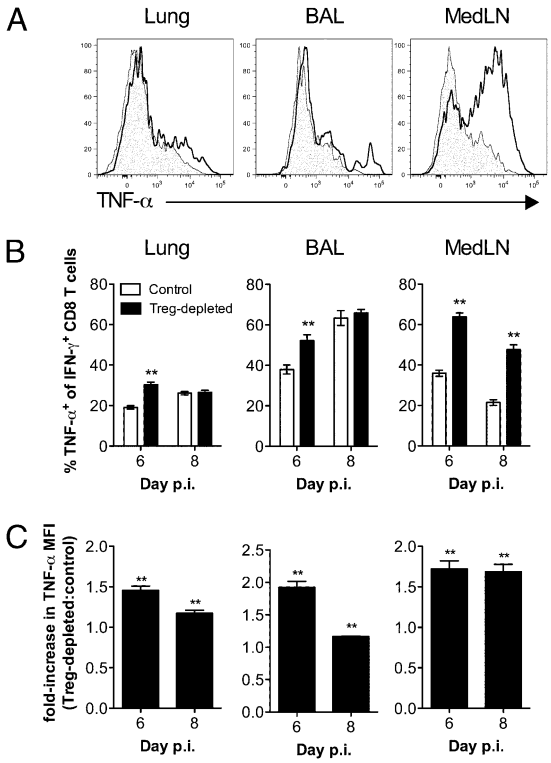

FIGURE 11. Increased TNF-α production by virus-specific CD8 T cells in the lungs, medLNs, and spleens of Treg-depleted mice. On days 6 and 8 p.i. cells from the lung parenchyma, BAL, and medLNs were stimulated directly ex vivo with $M2_{82–90}$ peptide and stained for intracellular IFN-γ and TNF-α. *A*, TNF-α production by $M2_{82–90}$-specific CD8 T cells on day 6 p.i. Histograms are gated on IFN-γ^+ CD8 T cells from control (gray shaded) or Treg-depleted mice (solid line). Histograms are representative of five separate experiments. *B*, Percentage of IFN-γ^+ CD8 T cells that coproduced TNF-α. *C*, Fold increase in the TNF-α geometric MFI in Treg-depleted mice over control mice. To calculate the fold increase, the geometric MFI was compared between groups within each experiment. Data in *B* and *C* represent the mean ± SEM from five experiments for day 6 p.i. and three experiments for day 8 p.i. with four mice per experiment. Data in *B* were analyzed using unpaired *t* tests. Data in *C* were analyzed using a two-way ANOVA on $\log_{10}$-transformed data. $*p < 0.05$; $**p < 0.01$.

However, there is little evidence that there is broad cross-reactivity between pathogen- and self-derived Ags. Furthermore, because Tregs have been shown to respond to a wide variety of pathogens, most of which establish chronic infections, cross-reactivity would have to be the rule rather than the exception. In a third scenario, nTregs may be nonspecifically activated through recognition receptors, such as TLRs, or cytokines, such as type I IFNs. Tregs express multiple TLRs, including TLR4, TLR5, TLR7, and TLR8 (48). This may be an intriguing possibility in the case of RSV infection since the RSV F protein has been shown to induce TLR4 signaling (49).

During certain conditions, Ag-specific adaptive Foxp3$^+$ CD4 regulatory T cells (aTregs) can be generated peripherally (5). Evidence for the development of aTregs is strongest at mucosal sites, such as the intestinal tract and the lungs (5, 11, 50). For example, intranasal delivery of Ag results in the conversion of conventional Foxp3$^-$ CD4 T cells into adaptive Foxp3$^+$ Tregs that can prevent allergic inflammation (11, 51). In response to pathogens, the generation of aTregs has been shown during persistent infections where Ag may be present in subimmunogenic conditions with low levels of inflammatory cytokines or low expression of costimulatory molecules (5). In contrast, acute infections may not provide the right type of environment that would require the additional regulation provided by aTregs (12). One major confounding issue in studying aTregs and nTregs is the lack of phenotypic markers to distinguish between the two populations. Consequently, in our studies we were unable to determine whether adaptive Foxp3$^+$ Tregs were contributing to the overall Treg response during acute RSV infection. There is evidence that a small frequency of Foxp3$^+$ Tregs in the lungs is RSV-specific as determined by tetramers (52). However, because the frequency of RSV-specific tetramer$^+$ CD4 T cells identified in this study was small (<1% of the total CD4 T cells in the lung), it is difficult to extrapolate what fraction of Foxp3$^+$ Tregs is RSV-specific. Unfortunately, without the ability to identify a larger proportion of RSV-specific CD4 T cells by tetramer and the lack of RSV-specific TCR transgenic mice, it is difficult at present to directly assess the generation of adaptive Foxp3$^+$ Tregs following acute RSV infection.

Foxp3$^+$ Tregs are commonly implicated in the suppression of the adaptive immune response to pathogens as a way to limit immunopathology. However, there is evidence that Tregs coordinate innate and adaptive immune responses to pathogens. Tregs have been reported to promote the trafficking of effector immune cells to the primary site of infection during genital HSV-2 infection (53) and in CB6F1 hybrid mice during RSV infection (21). Conversely, Tregs may also be able to block trafficking by inhibiting expression of chemokine receptors (54). During RSV infection in Treg-depleted CB6F1 mice, there was a significant lag in the $D^bM_{187–195}$-specific CD8 T cell responses in the lungs compared with control mice. This lag in the virus-specific T cell response corresponded with decreased virus clearance in the lungs on days 6 and 7 p.i. Our study substantiates this role of the Treg response in the BALB/c model. Importantly, our data offer the novel observation that there is an early accumulation of RSV-specific CD8 T cells in the lung-draining medLNs of Treg-depleted mice, suggesting that there is delayed egress out of the medLNs into the lungs. These findings suggest that Tregs help coordinate the early trafficking of activated CD8 T cells from the draining LNs into the lungs. Tregs may influence expression of chemokines in the lungs or chemokine receptors on virus-specific CD8 T cells. During RSV infection, CXCL10 has been shown to be important for the recruitment of virus-specific CD8 T cells into the lungs (55). Initial experiments did not reveal obvious differences in the chemokines CXCL9, CXCL10, CXCL11, CCL3, and CCL5 in the lung parenchyma and BAL as a whole (data not shown), but there may be more subtle differences in chemokines produced by specific immune cell populations. Alternatively, Tregs could influence expression levels of sphingosine 1–phosphate receptor 1 on CD8 T cells in the draining LNs, delaying their egress from the draining LNs into the lung. Our laboratory is currently examining these possibilities.

Much of what is known about RSV-induced pathogenesis comes from studies in the BALB/c mouse model (37, 56). In this study we demonstrated that depletion of CD25$^+$ Tregs prior to infection exacerbated disease severity. Given that we were only able to deplete ~60% of Foxp3$^+$ Tregs, we think that our results represent an underestimate of the overall effect that Tregs have in limiting pulmonary immunopathology. This study uniquely demonstrates that increased in vivo production of TNF-α by RSV-specific CD8 T cells could contribute to increased morbidity in Treg-depleted mice. Although there was no major increase in TNF-α production by CD8 T cells reported in Treg-depleted CB6F1 mice during RSV infection (21), we observed notable increases in ex vivo production of TNF-α by CD8 T cells in the lungs and medLNs of Treg-depleted mice. Although there were lower total numbers of $M2_{82–90}$-specific CD8 T cells in the lungs by day 6 p.i., this increase translated into significantly ($p < 0.001$) more total numbers of $M2_{82–90}$-specific CD8 T cells capable of coproducing IFN-γ and TNF-α in the

medLNs, a trend toward increased total numbers in the spleen ($p = 0.06$), and similar numbers in the lung (data not shown). Additionally, increased per cell production of TNF-α in Treg-depleted mice as indicated by MFI could further account for CD8 T cell-mediated disease.

RSV is the leading cause of severe lower respiratory virus infections in infants and is the second leading cause of virus-induced respiratory disease in the elderly and adults with chronic cardiopulmonary disorders or who are immunocompromised (57, 58). Although CD8 T cells are important in RSV clearance from the lungs, they may also contribute to disease pathology (59), but to what extent remains controversial (58). In addition to inhibiting autoimmunity to self-Ags, it is increasingly evident that Foxp3$^+$ Tregs have an important role in regulating the adaptive immune response to pathogens (12). By better understanding the function of Tregs during acute respiratory virus infections, we will gain further insight into the mechanisms in place to regulate virus-specific T cell responses. This may lead to the ability of the T cell response to be manipulated to optimize virus clearance while minimizing immunopathology. It is important to further expand these studies to other respiratory pathogens to better understand host–pathogen interactions and how Tregs regulate the immune response.

Acknowledgments

We thank Kevin Legge for critical review of the manuscript and Elizabeth Dastrup and Kathryn Chaloner for assistance with the statistical analyses. We also thank Stacey Hartwig for excellent technical assistance.

Disclosures

The authors have no financial conflicts of interest.

References

1. Holt, P. G., D. H. Strickland, M. E. Wikström, and F. L. Jahnsen. 2008. Regulation of immunological homeostasis in the respiratory tract. *Nat. Rev. Immunol.* 8: 142–152.
2. Wissinger, E. L., J. Saldana, A. Didierlaurent, and T. Hussell. 2008. Manipulation of acute inflammatory lung disease. *Mucosal Immunol.* 1: 265–278.
3. Raz, E. 2007. Organ-specific regulation of innate immunity. *Nat. Immunol.* 8: 3–4.
4. Lambrecht, B. N. 2006. Alveolar macrophage in the driver's seat. *Immunity* 24: 366–368.
5. Curotto de Lafaille, M. A., and J. J. Lafaille. 2009. Natural and adaptive Foxp3$^+$ regulatory T cells: more of the same or a division of labor? *Immunity* 30: 626–635.
6. Kim, J. M., J. P. Rasmussen, and A. Y. Rudensky. 2007. Regulatory T cells prevent catastrophic autoimmunity throughout the lifespan of mice. *Nat. Immunol.* 8: 191–197.
7. Hori, S., T. Nomura, and S. Sakaguchi. 2003. Control of regulatory T cell development by the transcription factor Foxp3. *Science* 299: 1057–1061.
8. Fontenot, J. D., M. A. Gavin, and A. Y. Rudensky. 2003. Foxp3 programs the development and function of CD4$^+$CD25$^+$ regulatory T cells. *Nat. Immunol.* 4: 330–336.
9. Wing, K., Y. Onishi, P. Prieto-Martin, T. Yamaguchi, M. Miyara, Z. Fehervari, T. Nomura, and S. Sakaguchi. 2008. CTLA-4 control over Foxp3$^+$ regulatory T cell function. *Science* 322: 271–275.
10. Rubtsov, Y. P., J. P. Rasmussen, E. Y. Chi, J. Fontenot, L. Castelli, X. Ye, P. Treuting, L. Siewe, A. Roers, W. R. Henderson, Jr., et al. 2008. Regulatory T cell-derived interleukin-10 limits inflammation at environmental interfaces. *Immunity* 28: 546–558.
11. Curotto de Lafaille, M. A., N. Kutchukhidze, S. Shen, Y. Ding, H. Yee, and J. J. Lafaille. 2008. Adaptive Foxp3$^+$ regulatory T cell-dependent and -independent control of allergic inflammation. *Immunity* 29: 114–126.
12. Wohlfert, E., and Y. Belkaid. 2008. Role of endogenous and induced regulatory T cells during infections. *J. Clin. Immunol.* 28: 707–715.
13. Rouse, B. T., P. P. Sarangi, and S. Suvas. 2006. Regulatory T cells in virus infections. *Immunol. Rev.* 212: 272–286.
14. Belkaid, Y., and B. T. Rouse. 2005. Natural regulatory T cells in infectious disease. *Nat. Immunol.* 6: 353–360.
15. Scott-Browne, J. P., S. Shafiani, G. Tucker-Heard, K. Ishida-Tsubota, J. D. Fontenot, A. Y. Rudensky, M. J. Bevan, and K. B. Urdahl. 2007. Expansion and function of Foxp3-expressing T regulatory cells during tuberculosis. *J. Exp. Med.* 204: 2159–2169.
16. Fulton, R. B., M. R. Olson, and S. M. Varga. 2008. Regulation of cytokine production by virus-specific CD8 T cells in the lungs. *J. Virol.* 82: 7799–7811.
17. Sakaguchi, S., N. Sakaguchi, M. Asano, M. Itoh, and M. Toda. 1995. Immunologic self-tolerance maintained by activated T cells expressing IL-2 receptor α-chains (CD25): breakdown of a single mechanism of self-tolerance causes various autoimmune diseases. *J. Immunol.* 155: 1151–1164.
18. Olson, M. R., S. M. Hartwig, and S. M. Varga. 2008. The number of respiratory syncytial virus (RSV)-specific memory CD8 T cells in the lung is critical for their ability to inhibit RSV vaccine-enhanced pulmonary eosinophilia. *J. Immunol.* 181: 7958–7968.
19. McKinley, L., A. J. Logar, F. McAllister, M. Zheng, C. Steele, and J. K. Kolls. 2006. Regulatory T cells dampen pulmonary inflammation and lung injury in an animal model of *Pneumocystis* pneumonia. *J. Immunol.* 177: 6215–6226.
20. Mills, K. H. 2004. Regulatory T cells: friend or foe in immunity to infection? *Nat. Rev. Immunol.* 4: 841–855.
21. Ruckwardt, T. J., K. L. Bonaparte, M. C. Nason, and B. S. Graham. 2009. Regulatory T cells promote early influx of CD8$^+$ T cells in the lungs of respiratory syncytial virus-infected mice and diminish immunodominance disparities. *J. Virol.* 83: 3019–3028.
22. Olson, M. R., and S. M. Varga. 2007. CD8 T cells inhibit respiratory syncytial virus (RSV) vaccine-enhanced disease. *J. Immunol.* 179: 5415–5424.
23. Nishioka, T., J. Shimizu, R. Iida, S. Yamazaki, and S. Sakaguchi. 2006. CD4$^+$ CD25$^+$Foxp3$^+$ T cells and CD4$^+$CD25$^-$Foxp3$^+$ T cells in aged mice. *J. Immunol.* 176: 6586–6593.
24. Lawrence, C. W., R. M. Ream, and T. J. Braciale. 2005. Frequency, specificity, and sites of expansion of CD8$^+$ T cells during primary pulmonary influenza virus infection. *J. Immunol.* 174: 5332–5340.
25. Taylor, M. D., A. Harris, S. A. Babayan, O. Bain, A. Culshaw, J. E. Allen, and R. M. Maizels. 2007. CTLA-4 and CD4$^+$CD25$^+$ regulatory T cells inhibit protective immunity to filarial parasites in vivo. *J. Immunol.* 179: 4626–4634.
26. Li, M. O., Y. Y. Wan, and R. A. Flavell. 2007. T cell-produced transforming growth factor-β1 controls T cell tolerance and regulates Th1- and Th17-cell differentiation. *Immunity* 26: 579–591.
27. Malek, T. R. 2008. The biology of interleukin-2. *Annu. Rev. Immunol.* 26: 453–479.
28. Fontenot, J. D., J. P. Rasmussen, M. A. Gavin, and A. Y. Rudensky. 2005. A function for interleukin 2 in Foxp3-expressing regulatory T cells. *Nat. Immunol.* 6: 1142–1151.
29. Fontenot, J. D., J. P. Rasmussen, L. M. Williams, J. L. Dooley, A. G. Farr, and A. Y. Rudensky. 2005. Regulatory T cell lineage specification by the forkhead transcription factor Foxp3. *Immunity* 22: 329–341.
30. Huehn, J., K. Siegmund, J. C. Lehmann, C. Siewert, U. Haubold, M. Feuerer, G. F. Debes, J. Lauber, O. Frey, G. K. Przybylski, et al. 2004. Developmental stage, phenotype, and migration distinguish naive- and effector/memory-like CD4$^+$ regulatory T cells. *J. Exp. Med.* 199: 303–313.
31. Friedline, R. H., D. S. Brown, H. Nguyen, H. Kornfeld, J. Lee, Y. Zhang, M. Appleby, S. D. Der, J. Kang, and C. A. Chambers. 2009. CD4$^+$ regulatory T cells require CTLA-4 for the maintenance of systemic tolerance. *J. Exp. Med.* 206: 421–434.
32. Takahashi, T., T. Tagami, S. Yamazaki, T. Uede, J. Shimizu, N. Sakaguchi, T. W. Mak, and S. Sakaguchi. 2000. Immunologic self-tolerance maintained by CD25$^+$CD4$^+$ regulatory T cells constitutively expressing cytotoxic T lymphocyte-associated antigen 4. *J. Exp. Med.* 192: 303–310.
33. Read, S., V. Malmström, and F. Powrie. 2000. Cytotoxic T lymphocyte-associated antigen 4 plays an essential role in the function of CD25$^+$CD4$^+$ regulatory cells that control intestinal inflammation. *J. Exp. Med.* 192: 295–302.
34. Lehmann, J., J. Huehn, M. de la Rosa, F. Maszyna, U. Kretschmer, V. Krenn, M. Brunner, A. Scheffold, and A. Hamann. 2002. Expression of the integrin $\alpha_E\beta_7$ identifies unique subsets of CD25$^+$ as well as CD25$^-$ regulatory T cells. *Proc. Natl. Acad. Sci. USA* 99: 13031–13036.
35. Xu, B., N. Wagner, L. N. Pham, V. Magno, Z. Shan, E. C. Butcher, and S. A. Michie. 2003. Lymphocyte homing to bronchus-associated lymphoid tissue (BALT) is mediated by L-selectin/PNAd, $\alpha_4\beta_1$ integrin/VCAM-1, and LFA-1 adhesion pathways. *J. Exp. Med.* 197: 1255–1267.
36. Belkaid, Y., C. A. Piccirillo, S. Mendez, E. M. Shevach, and D. L. Sacks. 2002. CD4$^+$CD25$^+$ regulatory T cells control *Leishmania major* persistence and immunity. *Nature* 420: 502–507.
37. Olson, M. R., and S. M. Varga. 2008. Pulmonary immunity and immunopathology: lessons from respiratory syncytial virus. *Expert Rev. Vaccines* 7: 1239–1255.
38. Graham, B. S., L. A. Bunton, P. F. Wright, and D. T. Karzon. 1991. Role of T lymphocyte subsets in the pathogenesis of primary infection and rechallenge with respiratory syncytial virus in mice. *J. Clin. Invest.* 88: 1026–1033.
39. Suvas, S., U. Kumaraguru, C. D. Pack, S. Lee, and B. T. Rouse. 2003. CD4$^+$ CD25$^+$ T cells regulate virus-specific primary and memory CD8$^+$ T cell responses. *J. Exp. Med.* 198: 889–901.
40. Haeryfar, S. M., R. J. DiPaolo, D. C. Tscharke, J. R. Bennink, and J. W. Yewdell. 2005. Regulatory T cells suppress CD8$^+$ T cell responses induced by direct priming and cross-priming and moderate immunodominance disparities. *J. Immunol.* 174: 3344–3351.
41. Rai, D., N. L. Pham, J. T. Harty, and V. P. Badovinac. 2009. Tracking the total CD8 T cell response to infection reveals substantial discordance in magnitude and kinetics between inbred and outbred hosts. *J. Immunol.* 183: 7672–7681.
42. Drake, D. R., III, R. M. Ream, C. W. Lawrence, and T. J. Braciale. 2005. Transient loss of MHC class I tetramer binding after CD8$^+$ T cell activation reflects altered T cell effector function. *J. Immunol.* 175: 1507–1515.
43. Rutigliano, J. A., and B. S. Graham. 2004. Prolonged production of TNF-α exacerbates illness during respiratory syncytial virus infection. *J. Immunol.* 173: 3408–3417.
44. McHugh, R. S., M. J. Whitters, C. A. Piccirillo, D. A. Young, E. M. Shevach, M. Collins, and M. C. Byrne. 2002. CD4$^+$CD25$^+$ immunoregulatory T cells: gene expression analysis reveals a functional role for the glucocorticoid-induced TNF receptor. *Immunity* 16: 311–323.

45. Banz, A., A. Peixoto, C. Pontoux, C. Cordier, B. Rocha, and M. Papiernik. 2003. A unique subpopulation of $CD4^+$ regulatory T cells controls wasting disease, IL-10 secretion and T cell homeostasis. *Eur. J. Immunol.* 33: 2419–2428.
46. Ito, T., S. Hanabuchi, Y. H. Wang, W. R. Park, K. Arima, L. Bover, F. X. Qin, M. Gilliet, and Y. J. Liu. 2008. Two functional subsets of $FOXP3^+$ regulatory T cells in human thymus and periphery. *Immunity* 28: 870–880.
47. Hsieh, C. S., Y. Liang, A. J. Tyznik, S. G. Self, D. Liggitt, and A. Y. Rudensky. 2004. Recognition of the peripheral self by naturally arising $CD25^+CD4^+$ T cell receptors. *Immunity* 21: 267–277.
48. Caramalho, I., T. Lopes-Carvalho, D. Ostler, S. Zelenay, M. Haury, and J. Demengeot. 2003. Regulatory T cells selectively express Toll-like receptors and are activated by lipopolysaccharide. *J. Exp. Med.* 197: 403–411.
49. Kurt-Jones, E. A., L. Popova, L. Kwinn, L. M. Haynes, L. P. Jones, R. A. Tripp, E. E. Walsh, M. W. Freeman, D. T. Golenbock, L. J. Anderson, and R. W. Finberg. 2000. Pattern recognition receptors TLR4 and CD14 mediate response to respiratory syncytial virus. *Nat. Immunol.* 1: 398–401.
50. Hall, J. A., N. Bouladoux, C. M. Sun, E. A. Wohlfert, R. B. Blank, Q. Zhu, M. E. Grigg, J. A. Berzofsky, and Y. Belkaid. 2008. Commensal DNA limits regulatory T cell conversion and is a natural adjuvant of intestinal immune responses. *Immunity* 29: 637–649.
51. Duan, W., T. So, and M. Croft. 2008. Antagonism of airway tolerance by endotoxin/lipopolysaccharide through promoting OX40L and suppressing antigen-specific $Foxp3^+$ T regulatory cells. *J. Immunol.* 181: 8650–8659.
52. Liu, J., T. J. Ruckwardt, M. Chen, T. R. Johnson, and B. S. Graham. 2009. Characterization of respiratory syncytial virus M- and M2-specific CD4 T cells in a murine model. *J. Virol.* 83: 4934–4941.
53. Lund, J. M., L. Hsing, T. T. Pham, and A. Y. Rudensky. 2008. Coordination of early protective immunity to viral infection by regulatory T cells. *Science* 320: 1220–1224.
54. Sarween, N., A. Chodos, C. Raykundalia, M. Khan, A. K. Abbas, and L. S. Walker. 2004. $CD4^+CD25^+$ cells controlling a pathogenic CD4 response inhibit cytokine differentiation, CXCR-3 expression, and tissue invasion. *J. Immunol.* 173: 2942–2951.
55. Lindell, D. M., T. E. Lane, and N. W. Lukacs. 2008. CXCL10/CXCR3-mediated responses promote immunity to respiratory syncytial virus infection by augmenting dendritic cell and $CD8(^+)$ T cell efficacy. *Eur. J. Immunol.* 38: 2168–2179.
56. Castilow, E. M., and S. M. Varga. 2008. Overcoming T cell-mediated immunopathology to achieve safe RSV vaccination. *Future Virol.* 3: 445–454.
57. Falsey, A. R., P. A. Hennessey, M. A. Formica, C. Cox, and E. E. Walsh. 2005. Respiratory syncytial virus infection in elderly and high-risk adults. *N. Engl. J. Med.* 352: 1749–1759.
58. Collins, P. L., and B. S. Graham. 2008. Viral and host factors in human respiratory syncytial virus pathogenesis. *J. Virol.* 82: 2040–2055.
59. Peebles, R. S., Jr., and B. S. Graham. 2005. Pathogenesis of respiratory syncytial virus infection in the murine model. *Proc. Am. Thorac. Soc.* 2: 110–115.